

## Solid state and solution fine tuning of the linear and non linear optical properties of (2-pyrene-1-yl-vinyl)pyridine by protonation/deprotonation reaction

E. Cariati,<sup>\*abc</sup> C. Botta,<sup>d</sup> S. G. Danelli,<sup>a</sup> A. Forni,<sup>\*c</sup> A. Giaretta,<sup>a</sup> U. Giovanella,<sup>d</sup> E. Lucenti,<sup>\*bc</sup> D. Marinotto,<sup>ab</sup> S. Righetto<sup>ab</sup> and R. Ugo<sup>ab</sup>

<sup>a</sup> Dipartimento di Chimica dell'Università degli Studi di Milano, via Golgi 19, 20133 Milano, Italy

<sup>b</sup> UdR INSTM di Milano, Via Golgi 19, 20133 Milano, Italy

<sup>c</sup> ISTM-CNR, Via Golgi 19, 20133 Milano, Italy

<sup>d</sup> ISMAC-CNR, Via Bassini 15, 20133 Milano, Italy

### Electronic Supplementary Information

#### Computational details

All calculations were performed with the Gaussian suite of programs.<sup>S1</sup>

The molecular structures of compounds **1** and (1H)<sup>+</sup> have been optimized in CHCl<sub>3</sub> within the DFT approach, using the 6-311++G(d,p) basis set and the PBE0 functional,<sup>S2,S3</sup> which was previously judged well suited for describing the electronic and optical features of a series of organic dyes.<sup>S4</sup>

Geometry optimization of **1** in chloroform gave a minimum structure slightly distorted from planarity (the dihedral angle between the pyrene and pyridine least-squares planes measures 35°), with a dipole moment of 4.41 D directed from pyridine to pyrene, while optimization of (1H)<sup>+</sup> in CHCl<sub>3</sub> gave an almost planar structure, with a dipole moment of 20.82 D directed from pyrene to pyridine.

Using the PBE0/6-311++G(d,p) optimized geometry, standard vertical Time Dependent (TD) DFT calculations<sup>S5-S7</sup> were carried out in CHCl<sub>3</sub> with the same basis set, to determine the excited state properties. Several functionals have been tested, that is, PBE0, CAM-B3LYP, LC-BLYP, M062X and  $\omega$ B97X, and the corresponding values of computed optical properties of **1** and (1H)<sup>+</sup> are reported in Table S1.

The different examined functionals provided very different values of absorption wavelengths and excited state dipole moments. The PBE0 functional was found to overestimate the values of the absorption wavelength, in particular as far as the protonated form is concerned, but correctly predicts a large increase of the dipole moment going from the ground to the excited state ( $\Delta\mu_{eg} = 7.07$  D), explaining the high hyperpolarizability of compound **1**. Moreover, it provides a lower oscillator strength for the protonated species with respect to the neutral one, as experimentally observed (see Figure 1, reporting the absorbance of **1** and (1H)<sup>+</sup> as measured in the

same solution before and after exposure to HCl vapours). On the other hand, the  $\omega$ B97X functional, though providing the better agreement with the absorption wavelengths, incorrectly predicts a too low  $\Delta\mu_{eg}$ , 3.00 D, and a higher oscillator strength for (1H)<sup>+</sup> with respect **1**. For these reasons we deemed the PBE0 functional more suitable to describe the optoelectronic features of the present compounds.

In all cases the major band predicted by TDDFT calculations principally corresponds to the HOMO  $\rightarrow$  LUMO transition, for both neutral and protonated species. The HOMO and LUMO were both  $\pi$  orbitals, the former principally localized on pyrene and the latter on pyridine (see a picture in Figs. S1 and S2).

In Figure S3 the electrostatic potential maps of the neutral and protonated species in both the ground and the excited states are reported, showing an increased polarization for the former and the opposite for the latter species.

**Table S1.** Computed electronic transitions ( $\lambda_{max}$ , nm), along with the associated excited state dipole moments ( $\mu_e$ , D), the difference between the dipole moment moduli of the excited and ground states ( $\Delta\mu_{eg}$ , D), the transition dipole moments ( $\mu_{eg}$ , D) and the oscillator strengths ( $f$ ), for compounds **1** and (1H)<sup>+</sup> using different functionals.<sup>a</sup>

Functional	$\lambda_{max}$	$\mu_e$	$\Delta\mu_{eg}$	$\mu_{eg}$	$f$
<b>1</b>					
PBE0	426	11.48	7.07	10.64	1.27
M062X	386	9.12	4.71	10.72	1.43
CAM-B3LYP	388	8.76	4.35	10.74	1.44
$\omega$ B97X	366	7.41	3.00	10.66	1.51
LC-BLYP	354	7.20	2.79	10.54	1.54
Exp	378				
<b>(1H)<sup>+</sup></b>					
PBE0	562	8.93	-11.89	11.90	1.19
M062X	498	9.17	-11.65	12.10	1.38
CAM-B3LYP	495	9.57	-11.25	12.24	1.43
$\omega$ B97X	454	10.95	-9.87	12.23	1.56
LC-BLYP	436	11.24	-9.58	12.18	1.60
Exp	443				

<sup>a</sup>Electronic transitions computed in CHCl<sub>3</sub> with the 6-311++G(d,p) basis set using the TDDFT formalism. The values of  $\Delta\mu_{eg}$  are computed using the ground state dipole moment obtained at PBE0/6-311++G(d,p) level, 4.41 D for **1** and 20.82 D for (1H)<sup>+</sup>.

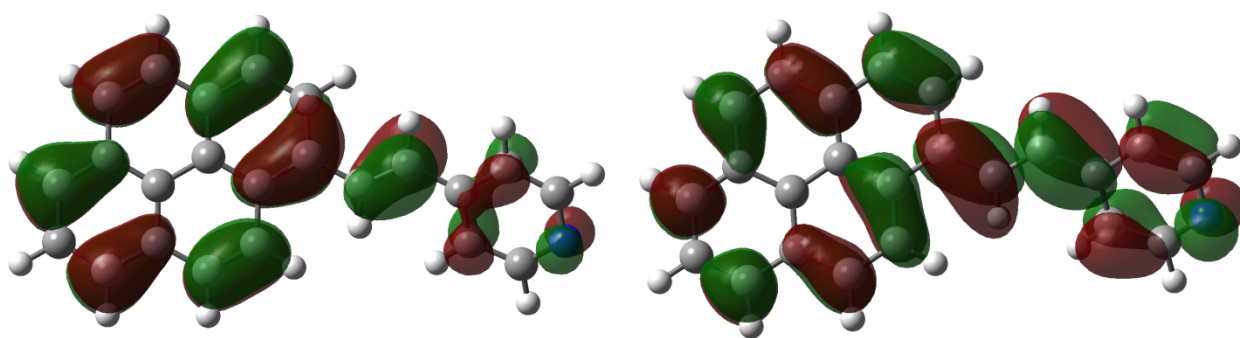


**Fig. S1.** Plots of the PBE0/6-311++G\*\* HOMO (left) and LUMO (right) of compound **1** in  $\text{CHCl}_3$ . Isosurfaces value 0.02.

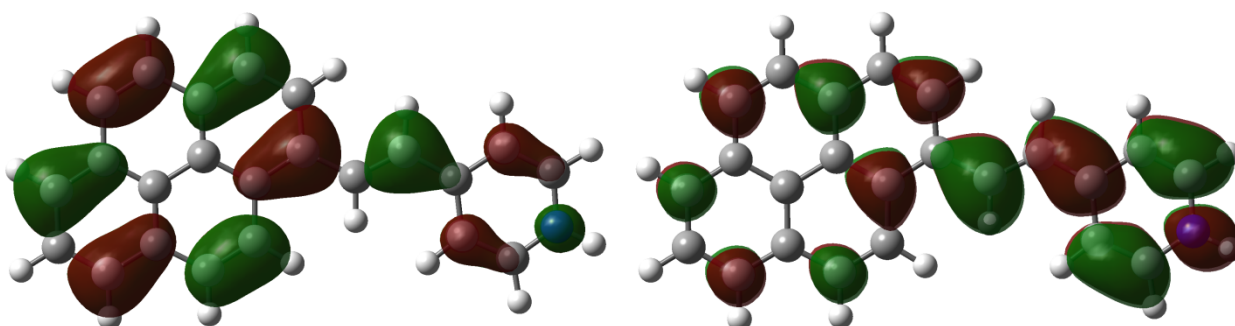


**Fig. S2.** Plots of the PBE0/6-311++G\*\* HOMO (left) and LUMO (right) of compound  $(\mathbf{1H})^+$  in  $\text{CHCl}_3$ . Isosurfaces value 0.02.

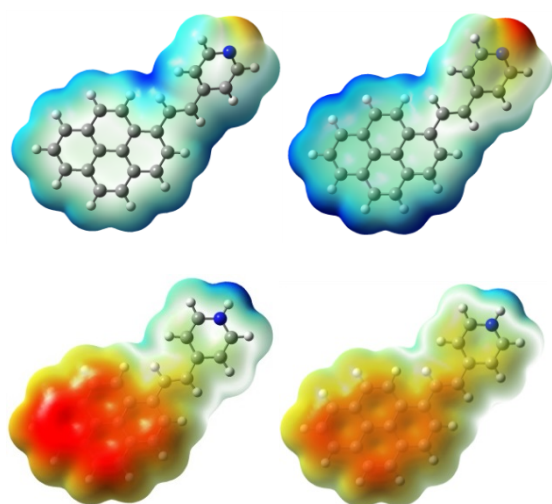


**Fig. S3.** Plots of the electrostatic potentials of the ground (left) and the excited states (right), computed at PBE0/6-311++G(d,p) and TD-PBE0/6-311++G(d,p) levels, respectively) of compounds **1** (above) and  $(\mathbf{1H})^+$  (below), mapped on the respective isosurfaces (0.001 a.u.) of electron density. Values of electrostatic potential range from -0.08 (red) to 0.04 (blue) a.u. for **1** and from 0.06 (red) to 0.18 (blue) a.u. for  $(\mathbf{1H})^+$ .

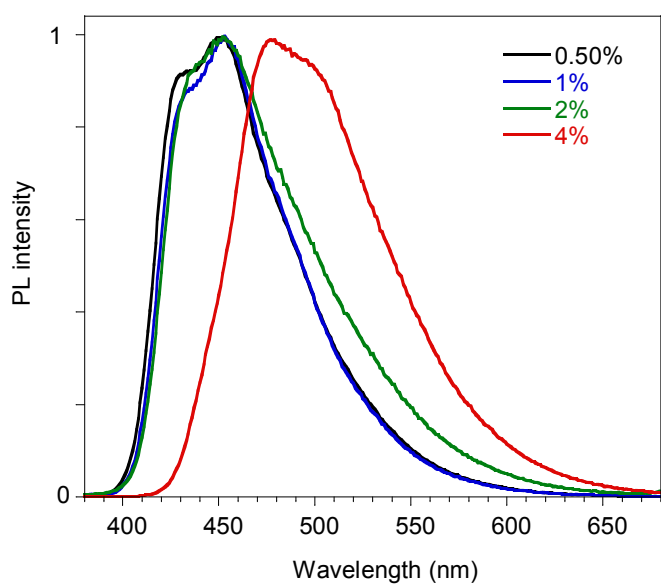


**Fig. S4.** Emission spectra of film 1/PMMA at different dye loadings.

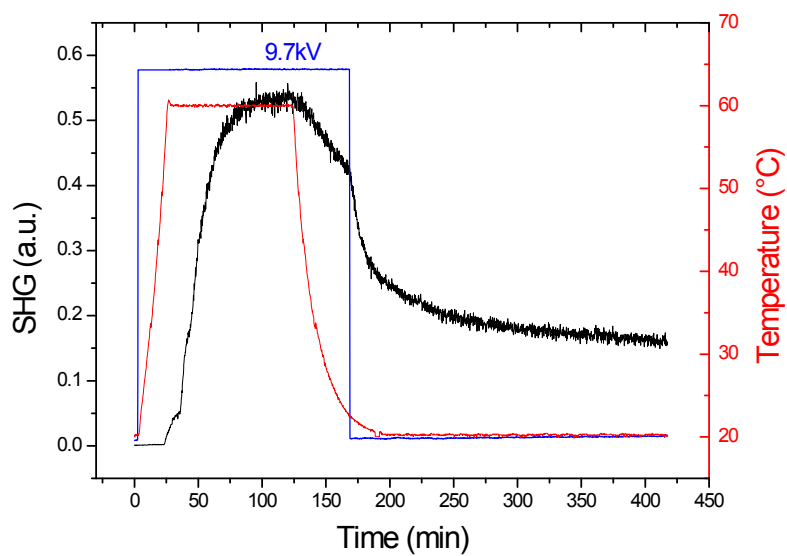


**Fig. S5.** SHG response of film 1/PMMA poled at 60°C.

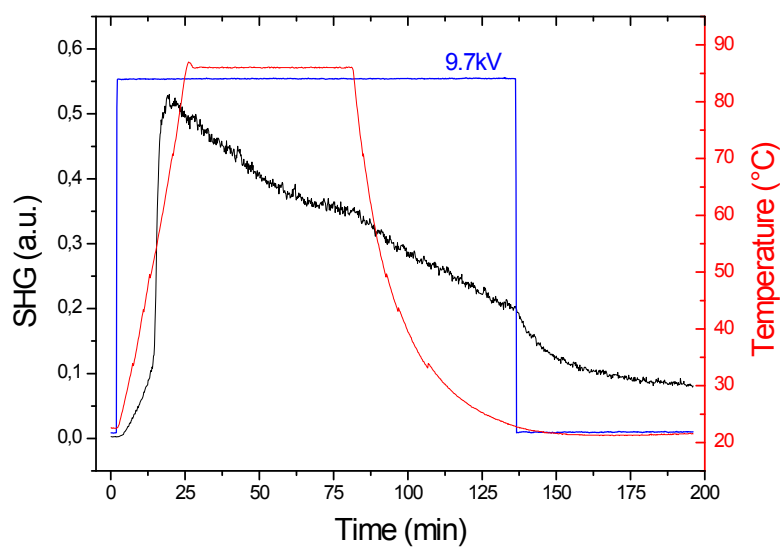


**Fig. S6.** SHG response of film 1/PMMA poled at 85°C.

**Table S2.** 1/PMMA film thickness measured by profilometry (Bruker DektakXT instrument)

	Pristine	After exposure to HCl vapours (60 s)	After exposure to NH <sub>3</sub> vapours (30 s)	After cycles 12	After cycles 18
<b>Film thickness (μm)</b>	2.010 ± 0.100	1.930 ± 0.095	2.057 ± 0.070	2.260 ± 0.160	2.050 ± 0.080

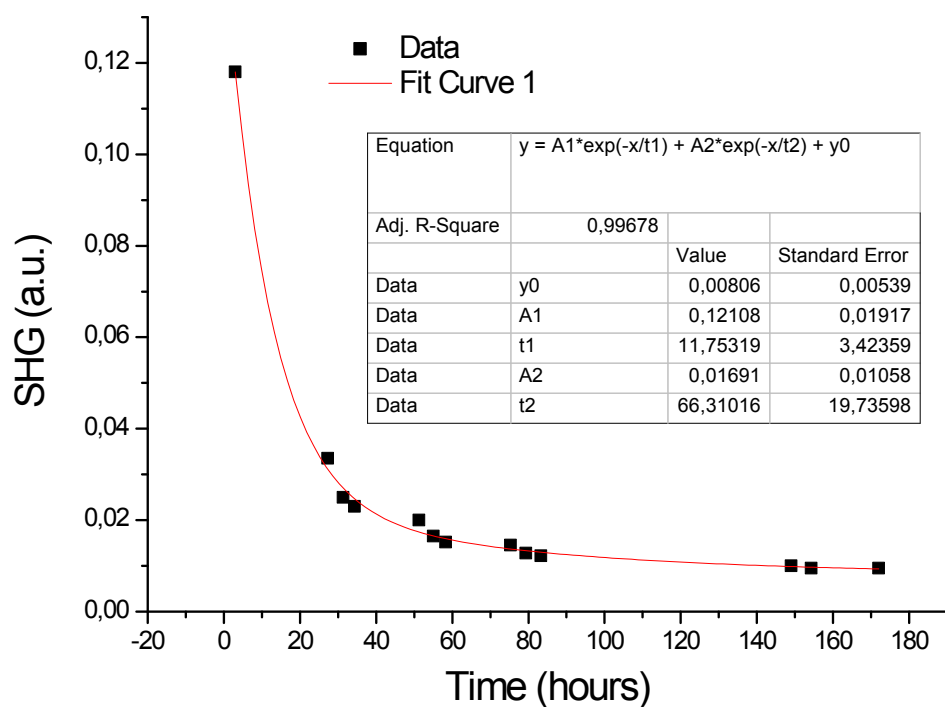


**Fig. S7.** Decay of the SHG signal of film 1/PMMA after poling at 60°C.

The whole trend of decay in the time of the SHG signal was fitted by a double exponential function taking into account also the persistence, just after the switch off of the electric field, of surface charges resulting from the formation of ions on the film surface during the corona poling process (equation reported in the inset of Figure S7).  $t1$  and  $t2$  are, respectively, the fast, just after the switch off of the electric field, and slow relaxation times of the NLO chromophore reorientation within the polymeric matrix. In particular,  $t1$  is the relaxation time due to their rotational reorientation within the free volumes of the microscopic network of the polymer in the presence of surface charges, an effect which disappears in few hours, and  $t2$  is the relaxation time mainly due to the chromophore reorientation originating from the segmental mobility of PMMA.<sup>S8</sup>

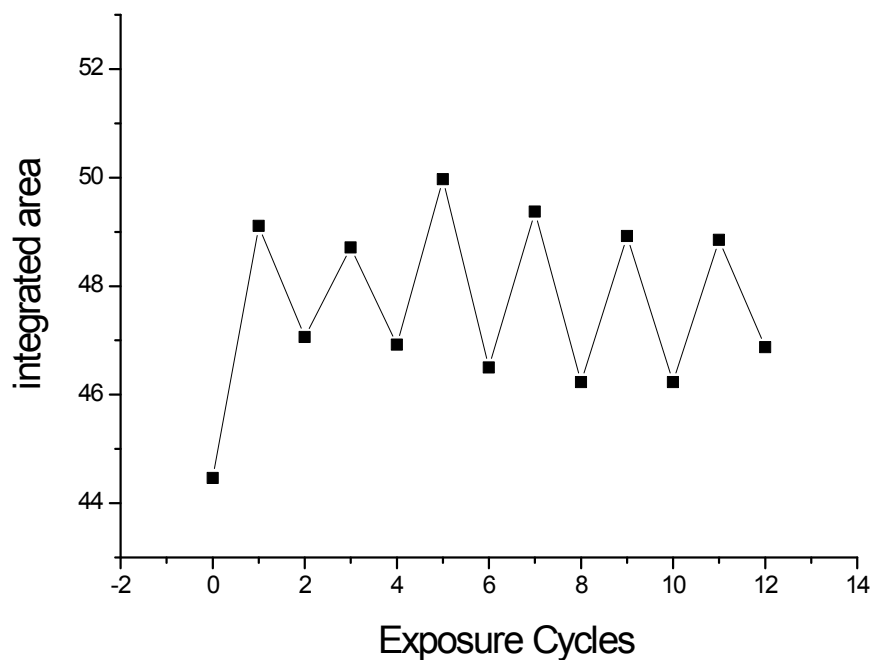
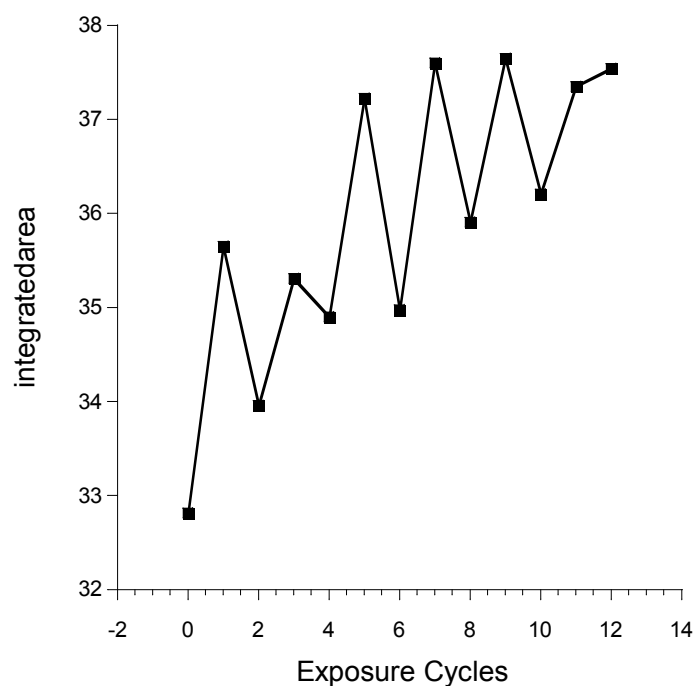


**Fig. S8.** Integrated area under absorption spectra recorded at  $0^\circ$  (top) and  $60^\circ$  (bottom) with unpolarized light after each cycle

The trend of the integrated area indicates a loss of orientation of the chromophore during the switches and well correlates with the loss of SHG signal observed.

## References

- S1 *Gaussian 09, Revision B.01*, M. J. Frisch *et al.*, Gaussian, Inc., Wallingford CT, 2010.
- S2 M. Ernzerhof and G. E. Scuseria, *J. Chem. Phys.*, 1999, **110**, 5029.
- S3 C. Adamo and V. Barone, *J. Chem. Phys.*, 1999, **110**, 6158.
- S4 D. Jacquemin, E. A. Perpète, G. E. Scuseria, I. Ciofini and C. Adamo, *J. Chem. Theory Comput.*, 2008, **4**, 123; D. Jacquemin, V. Wathélet, E. A. Perpète and C. Adamo, *J. Chem. Theory Comput.*, 2009, **5**, 2420; D. Jacquemin, A. Planchat, C. Adamo and B. Mennucci, *J. Chem. Theory Comput.* 2012, **8**, 2359–2372.
- S5 E. Runge and E. K. U. Gross, *Phys. Rev. Lett.* 1984, **52**, 997.
- S6 R. E. Stratmann, G. E. Scuseria and M. J. Frisch, *J. Chem. Phys.*, 1998, **109**, 8218.
- S7 M. E. Casida, *J. Mol. Struct. (THEOCHEM)*, 2009, **914**, 3.
- S8 T. Goodson III and C. H. Wang, *Macromolecules*, 1993, **26**, 1837; P. C. Ray and P. K. Das, *Eur. Polym. J.*, 1996, **32**, 51; M. Casalboni, F. Sarcinelli, R. Pizzoferrato, R. D'Amato, A. Furlani and M. V. Russo, *Chem. Phys. Lett.*, 2000, **319**, 107.